

CREEP SLUMP IN GLACIER RESERVOIRS—THEORY AND EXPERIMENT

By E. M. SHOEMAKER

(Faculty of Science, Simon Fraser University, Burnaby, British Columbia V5A 1S6, Canada)

ABSTRACT. Frequently the reservoir region of a cold surge-type glacier has a temperate base, while in a region surrounding the reservoir the base is cold. We analyse the slump process in such a reservoir region—that is, the process whereby material flows toward the lower end of the region and forms a critical wave profile there. The model agrees qualitatively with observations of Trapridge Glacier, Yukon Territory, Canada, which is currently experiencing a critical pre-surge condition. Calculations based on the model give good agreement with the surge cycle time of Rusty Glacier, Yukon Territory. Laboratory experiments show that a large-amplitude slump-induced wave profile forms prior to a surge. Experimental surges were produced with velocity increases of order one hundred.

RÉSUMÉ. Vidange brutale de bassins glaciaires. Théorie et expérience. Fréquemment le bassin d'alimentation d'un glacier froid du type à crue possède un fond tempéré tandis que, dans les zones entourant le bassin le fond est froid. Nous analysons le processus de vidange d'un tel bassin, c'est-à-dire le processus par lequel le matériel s'écoule vers le point bas du bassin et y forme une onde de crue critique. Le modèle est qualitativement en accord avec les observations faites sur le Trapridge Glacier, dans le territoire du Yukon au Canada, qui se trouve souvent en conditions critiques de pré-crue. Des calculs basés sur le modèle donnent un bon accord avec la période de la crue cyclique du Rusty Glacier dans le territoire du Yukon. Des expériences de laboratoire montrent qu'une vidange de grande amplitude provoque un profil ondulé préalablement à la crue. On a produit des crues expérimentales avec des accroissements de vitesse de l'ordre de un cent.

ZUSAMMENFASSUNG. Kriech-Einbrüche in Gletscher-Nährgebieten — Theorie und Versuch. Häufig hat das Nährgebiet eines kalten ausbrechenden Gletschers einen temperierten Untergrund, während in einem Bereich um das Nährgebiet der Untergrund kalt ist. Die vorliegende Analyse gilt dem Einbruchsprozess in einem solchen Nährgebiet, d.h. jenem Prozess, bei dem Material gegen das untere Ende des Gebietes fließt und dort ein kritisches Wellenprofil bildet. Das Modell stimmt qualitativ mit Beobachtungen am Trapridge Glacier, Yukon Territory, Kanada, überein, der derzeit eine kritische Vor-Ausbruchs-Phase durchläuft. Berechnungen auf der Basis des Modells geben gute Übereinstimmung mit dem Ausbruchszyklus des Rusty Glacier, Yukon Territory. Laborversuche zeigen, dass sich vor einem Ausbruch ein Wellenprofil mit grosser Amplitude, hervorgerufen durch einen Einbruch, bildet. Experimentell wurden Ausbrüche mit Geschwindigkeitsanstiegen bis zum Hundertfachen erzeugt.

INTRODUCTION

Although the majority of surge-type glaciers may be temperate, most of those which Clarke (1976), in his discussion of a thermal instability mechanism of surge, classified according to their thermal regime, are cold glaciers. Regarding these, Clarke states: "Only two cold surge-type glaciers, the Rusty and Trapridge in the Yukon Territory, have a reasonably well-known thermal structure." This thermal structure is of a type which we believe is common to most cold surge-type glaciers. We shall term glaciers of this type cold-temperate-cold (ctc). In a ctc glacier a large central region with a temperate base is surrounded by ice with a cold base. Generally the ice is cold except at the central base.*

Following the terminology first employed by Meier and Post (1969) we shall term the central region the reservoir region. This study will be concerned with the transient flow in this region. It is clear that since sliding can occur in the reservoir region but not in the bounding regions, as time increases there will be a displacement of material from the upper towards the lower region of the reservoir. Such a process is commonly termed slump.†

* In his original consideration of the thermal instability mechanism of glacier surge, Robin (1955) suggested that basal ice is melted by internal friction. We think it more likely that the greater ice thickness of the central region which insulates the base from the surface cold source, coupled with bottom geothermal heating, is the cause of melting.

† For a description of slump in a glacier see Collins's (1972) remarks regarding Trapridge Glacier along with our remarks under Field observations below. Slump is also of importance in rock mechanics where it is analysed under assumptions very different from those employed here (Scheidegger, 1975, p. 129).

Our purpose is to study the slump process as it leads to a pre-surge condition. This involves the definition of a critical pre-surge condition and determination of the development of this condition and its dependence upon geometry, temperature, and time. This objective is attained by an analytical study based upon a linear flow law in which the effect of side drag is included but basal drag is neglected. The analytical model is compared qualitatively with the recent behaviour of Trapridge Glacier, which is currently experiencing a pre-surge condition, and quantitatively with Rusty Glacier, for which the necessary data exist. Finally, experimental results from a laboratory model are compared qualitatively with the analytical model and with the behaviour of Trapridge Glacier.

ANALYTICAL MODEL

The model is based upon a rectangular channel of width w , slope δ , and constant length l (Fig. 1) where accumulation, ablation, and material transfer across the ends of the channel are neglected.* Neglect of basal drag implies that shear flow is neglected in planes parallel to the xy plane (Fig. 1).† We assume additionally that material elements travel in planes parallel to the xz plane. Side drag cannot be neglected, because of cold marginal ice, and is assumed to result from a parabolic velocity profile across any section $x = \text{constant}$, an assumption consistent with a linearized flow law and fully developed laminar flow. Finally, we assume homogeneous material properties so that temperature is averaged. We wish to determine the development of the reservoir profile $h(x, y, t)$ where $h(x, y, 0) = h_0$, a constant.‡

The model reservoir is essentially a rectangular tank of uniform viscous fluid, lubricated base and unlubricated sides, placed in an inclined plane. Slump is a gravity-induced flow in which the free-surface moves from its initial position parallel to the plane towards a horizontal position. The model is concerned with the transient configuration, long before the final position is approached.

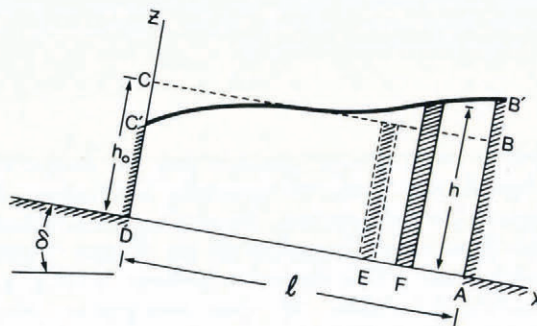


Fig. 1. The reservoir region is of fixed length l and initial height h_0 . Assumptions imply that a rectangular element on the centre line at E flows into a rectangular element at F . This flow produces a profile $C'B'$ at some later time.

* The primary effect of material flow across the channel ends is the localized effect shown in Figure 3. Velocities of order 2–5 m/year which exist above the reservoirs on Trapridge and Rusty Glaciers can be shown to be negligible in their influence upon the critical slump time of a reservoir since the input of material at the upper end can reduce length l in the analysis by only a negligible amount over the time period of critical slump. Normally, output velocities at the lower end of a reservoir are very small.

† The author's current results show that if the sliding resistance is reduced in a central region, the ratio of basal shear stress τ_b to deviatoric stress s_x satisfies $|\tau_b/s_x| \ll 1$ on average in the region during the early stages of transient adjustment to the changed boundary condition. This result justifies the neglect of shear stress in the reservoir region. Morland and Johnson (1980) showed that $|\tau_b/s_x| \gg 1$ in ice sheets under constant state conditions and a uniform sliding law.

‡ The assumption of initial constant depth is made for the sake of convenience and reasonableness. The qualitative results will not be affected by any particular choice of initial condition, although critical slump times will be dependent.

Some preliminary discussion of the relationship of this problem to the surge cycle of a ctc glacier would appear to be appropriate. Subsequent to a surge the advection of cold ice to lower depths and the general diminution of internal heat dissipation combine to produce a cold reservoir base. There follows a relatively long quiescent period during which the ablation region below the reservoir melts back and enters a dormant state while the reservoir undergoes accumulation and is in an inactive state. As the accumulation phase proceeds, basal melting is initiated and spreads. Later, increased crevassing at the upper end of the reservoir and slope steepening at the lower end are two characteristics, noted by many, of a pre-surge condition. Our conjecture is that the slope steepening is a manifestation of slump and is part of the surge-triggering mechanism for a ctc glacier. (This conclusion is reinforced by experimental results. See later.) Our object here is to investigate only the pre-surge slump process, although we must (arbitrarily) terminate the pre-surge process by defining a "critical" slump condition which marks the onset of lower reservoir instability.

Consideration of the equilibrium of an element bounded by planes $z = 0$, $x = x$, $x = x + \Delta x$, $y = y$, $y = y + \Delta y$ and the free surface $h(x, y, t)$ yields the equation

$$(\partial/\partial x)(h\sigma_x) + (\partial/\partial y)(\tau_{xy}h) + \rho gh \sin \delta = 0 \tag{1}$$

where σ_x is the normal stress in the x -direction averaged across thickness h , and τ_{xy} the shear stress on a plane $y = \text{const}$ which is z -independent from previous assumptions. The tensorial flow law

$$s_{ij} = 2\mu\dot{\epsilon}_{ij} \tag{2}$$

where s_{ij} and $\dot{\epsilon}_{ij}$ are, respectively, the stress and strain-rate deviators, gives

$$\tau_{xy} = \mu(\partial v/\partial y) \tag{3}$$

where $v(x, y, t)$ is the x -component of velocity. (The z -component is neglected.)

The assumed parabolic velocity profile

$$v(x, y, t) = V(x, t)(1 - 4y^2/w^2) \tag{4}$$

where V is the centre-line velocity, along with Equation (3), gives on the centre line

$$\frac{\partial}{\partial y}(\tau_{xy}h) = \frac{-8\mu}{w^2} h(x, t)V(x, t). \tag{5}$$

By definition

$$\sigma_x = s_x + \frac{1}{3}(\sigma_x + \sigma_y + \sigma_z), \tag{6}$$

and as a consequence of plane flow

$$\sigma_y = \frac{1}{2}(\sigma_x + \sigma_z). \tag{7}$$

Assuming that σ_z is unaffected by the flow field so that $\sigma_z = (-\rho g \cos \delta)(h - z)$, the stress σ_z averaged through thickness h is

$$\sigma_z = (-\rho gh \cos \delta)/2. \tag{8}$$

Equations (6), (7), and (8) combine to give

$$\sigma_x = 2s_x - (\rho gh \cos \delta)/2. \tag{9}$$

Normal strains will become large near the ends of the reservoir. For this reason Equation (2) is amended in its x -component by replacing $\dot{\epsilon}_x = \partial v/\partial x$ by a logarithmic strain measure* defined by

$$E_x = \ln(1 + \epsilon_x), \tag{10}$$

* The logarithmic strain measure is introduced only for the one strain component which becomes large. The other strain components will remain small throughout. For example, shear strains approach zero in the reservoir end regions since $V \rightarrow 0$.

so that

$$\dot{E}_x = \dot{\epsilon}_x / (1 + \epsilon_x). \quad (11)$$

Equations (9), (2), and (11) now combine to give on the centre line*

$$\frac{\partial}{\partial x} (h\sigma_x) = 4\mu \frac{\partial}{\partial x} \left[\left\{ h(x, t) \frac{\partial V(x, t)}{\partial x} \right\} / \left\{ 1 + \int_0^t \frac{\partial V(x, \xi)}{\partial x} d\xi \right\} \right] - (\rho g \cos \delta) h(x, t) \frac{\partial}{\partial x} h(x, t). \quad (12)$$

Substitution of Equations (5) and (12) into Equation (1) gives the centre-line equilibrium equation

$$4\mu \frac{\partial}{\partial x} \left[h \frac{\partial V}{\partial x} / \left\{ 1 + \int_0^t \frac{\partial V}{\partial x} dt \right\} \right] - (\rho g \cos \delta) h \frac{\partial h}{\partial x} - \frac{8\mu}{w^2} hV + (\rho g \sin \delta) h = 0. \quad (13)$$

Consideration of material conservation for a rectangular element on the centre line results in

$$(\partial/\partial x)(hV) + \partial h/\partial t = 0. \quad (14)$$

The system (13), (14), although non-linear, has much in common with linear second-order parabolic equations such as the heat equation. This will become apparent when a numerical solution is considered. The appropriate side conditions are

$$h(x, 0) = h_0, \quad 0 \leq x \leq l, \quad (15)$$

$$V(0, t) = V(l, t) = 0, \quad t \geq 0. \quad (16)$$

Dimensionless time, geometry, and velocity variables are introduced as follows:

$$\tau = (\rho g l \sin \delta / 8\mu) t, \quad (17)$$

$$\alpha = x/l, \quad \eta = h/h_0, \quad r = w/l, \quad s = h_0 \cot \delta/l, \quad (18)$$

$$U = 8\mu V / \rho g w^2 \sin \delta. \quad (19)$$

The variable τ is suggested by the analysis of one-dimensional creep rupture as done by Hoff (1953). Thus, a uniform linear viscous bar subjected to a nominal tensile stress σ_0 , with strain measured by E_x in Equation (10) will neck down to zero cross-sectional area within the "creep rupture time"

$$t_c = 4\mu/\sigma_0. \quad (20)$$

In the present problem, if side drag is neglected, the nominal stress magnitude at $x = 0$ and $x = l$ is

$$\sigma_0 = -\rho g l \sin \delta/2. \quad (21)$$

Considering Equations (17), (20), and (21) we see that the creep rupture time corresponding to σ_0 in Equation (21) is $\tau_c = 1$.

* The term $\int_0^t [\partial V(x, \xi)/\partial x] d\xi$ integrates strain-rate at a fixed point in space and therefore is only an approximation to what should actually be expressed, the integral of strain-rate following a particle. The approximation was introduced for a necessary computational simplification. Computations were made using a "correct" Lagrangian frame-indifferent formulation and compared with the present formulation for the special case of zero side drag; no discernible errors were encountered. Note that strain-rates are high only in the end regions where displacements are small, thus minimizing any error in approximation of the material derivative by $\partial V/\partial x$.

The dimensionless form of Equations (13) and (14), utilizing Equations (17), (18), and (19), becomes

$$\frac{r^2}{2} \frac{\partial}{\partial \alpha} \left[\eta \frac{\partial U}{\partial \alpha} / \left\{ 1 + r^2 \int_0^\tau \frac{\partial U}{\partial \alpha} d\tau \right\} \right] - s\eta(\partial\eta/\partial\alpha) - \eta U + \eta = 0, \tag{22}$$

$$r^2(\partial/\partial\alpha)(\eta U) + \partial\eta/\partial\tau = 0, \tag{23}$$

with Equations (15) and (16) transformed to

$$\eta(\alpha, 0) = 1, \quad 0 \leq \alpha \leq 1, \tag{24}$$

$$U(0, \tau) = U(1, \tau) = 0, \quad \tau \geq 0. \tag{25}$$

The slump process for the model is thus governed by the two parameters r and s defined in Equation (18). Parameter r will be termed the drag parameter. For $r \rightarrow \infty$ side drag is absent; ctc reservoirs appear to give r values in the range $0.2 < r < 0.6$. The term in Equation (22) involving parameter s exists from Equations (6) and (9) as a result of the change with respect to α of hydrostatic stress; we will term s the hydrostatic variation parameter. This parameter appears to lie near the range $0.2 < s < 0.5$ for ctc reservoirs. It will become clear that increased s results in increased drag. The first term of Equation (22) represents deformation due to longitudinal stresses with drag absent; the fourth term represents the imposed gravitational body force.

ANALYTICAL RESULTS

A finite-difference scheme is employed on a uniform rectangular mesh with Equations (22) and (23) approximated by

$$(r^2/2)(d^2/d\alpha^2) U(\alpha, 0) - U(\alpha, 0) + 1 = 0, \tag{26'}$$

$$\begin{aligned} & \frac{r^2}{2} \left[\frac{d}{d\alpha} \left(\eta(\alpha, \tau + \Delta\tau) \frac{d}{d\alpha} U(\alpha, \tau + \Delta\tau) \right) \right] / \left[1 + r^2 \int_0^\tau \frac{d}{d\alpha} U(\alpha, \xi) d\xi \right] - \\ & - \frac{r^4}{2} \left[\left\{ \int_0^\tau \frac{d^2}{d\alpha^2} U(\alpha, \xi) d\xi \right\} \eta(\alpha, \tau + \Delta\tau) \frac{dU}{d\alpha}(\alpha, \tau + \Delta\tau) \right] / \left[1 + r^2 \int_0^\tau \frac{d}{d\alpha} U(\alpha, \xi) d\xi \right]^2 - \\ & - s\eta(\alpha, \tau + \Delta\tau) \frac{d}{d\alpha} \eta(\alpha, \tau + \Delta\tau) - \eta(\alpha, \tau + \Delta\tau) U(\alpha, \tau + \Delta\tau) + \\ & + \eta(\alpha, \tau + \Delta\tau) = 0, \tag{26} \end{aligned}$$

$$\eta(\alpha, \Delta\tau) = 1 - r^2 \frac{d}{d\alpha} U(\alpha, 0) \Delta\tau, \tag{27'}$$

$$\eta(\alpha, \tau + \Delta\tau) = \eta(\alpha, \tau - \Delta\tau) - r^2 \left(\frac{d}{d\alpha} \eta(\alpha, \tau) U(\alpha, \tau) \right) (2\Delta\tau), \tag{27}$$

where $\tau = 0, \Delta\tau, 2\Delta\tau, \dots, \alpha = 0, \Delta\alpha, 2\Delta\alpha, \dots, n\Delta\alpha = 1$. The procedure is: (a) solve Equation (26') for the initial velocity $U(\alpha, 0)$; (b) solve Equation (27') for $\eta(\alpha, \Delta\tau)$; (c) solve Equation (26) for $U(\alpha, \Delta\tau)$; (d) solve Equation (27) for $\eta(\alpha, 2\Delta\tau)$, etc.

Equation (27) is a simple explicit difference formula while Equations (25) and (26) represent a two-point boundary-value problem for a linear second-order ordinary differential equation. The boundary conditions (25) are satisfied by employing a shooting method (Keller, 1968); in this case because Equation (26) is linear the shooting method is explicit, i.e. no iteration is required.

Note that a change in a function value $\eta(\alpha, \tau)$ or $U(\alpha, \tau)$ affects the value of $\eta(\alpha, \tau + \Delta\tau)$ through Equation (27) which, in turn, affects all the values $U(\alpha, \tau + \Delta\tau)$, $\alpha = \Delta\alpha, 2\Delta\alpha, \dots$ through Equation (26). Thus, the domain of dependence of a point $(\alpha, \tau + \Delta\tau)$ is the entire interval (α, τ) , $0 < \alpha < 1$. This fact helps to alleviate apprehension that the difference scheme might be unstable because the system is parabolic (Isaacson and Keller, 1966, p. 501-12). In practice, instability was not encountered. Three-place accuracy, using either single or double precision arithmetic, was achieved for the results in Figure 2 with $\Delta\alpha = 0.01$ and $\Delta\tau$ ranging from 0.001 for small s to 0.000 015 for large s .*

Figure 2 graphs dimensionless critical slump time τ_c versus r for various values of s , where critical slump is (arbitrarily) defined as an average thickening at the lower reservoir end of 30%. The actual physical end constraint could be expected to reduce this 30% thickening, perhaps to 20% as depicted in Figure 3, a value which appears reasonable as corresponding to a surge initiation condition for a glacier.†

Letting η_c represent the average dimensionless critical reservoir height at the lower end it is easily shown‡ that

$$\eta_c = \int_0^1 \frac{d\beta}{\beta^2 + (1-\beta^2)/\eta(1, 0, \tau_c)} = \frac{\eta}{(\eta-1)^{\frac{1}{2}}} \tan^{-1}(\eta-1)^{\frac{1}{2}}. \quad (28)$$

Thus, with $\eta_c = 1.3$, $\eta(1, 0, \tau_c)$ is 1.490 from Equation (28), the right-hand intercept of the curves in Figure 3.

Figure 2 shows that, as expected, the slump process, as measured by τ_c , is slowed by increasing drag (decreasing r); however, the drag effect is only moderate for $r > 0.2$. For $r < 0.2$ the curves increase rapidly. We expect that surge-type glaciers will lie in the range $r > 0.2$. The drag effect would not be expected to be more pronounced for a non-linear flow law. The effect upon τ_c of hydrostatic variation as measured by s is also moderate throughout the r and s range depicted but it is clear that as s increases beyond unity τ_c increases rapidly. (The moderate effect of side drag upon τ_c is another justification for neglecting basal drag.)

Figure 2 also shows various discrete values corresponding to a linearized strain measure ϵ_x in place of Equation (10). The effect is a decrease in τ_c values§ of order 20%.

Figure 3 plots critical reservoir centre-line profiles $\eta(\alpha, 0, \tau_c)$ for various r values and $s = 0$, with interpretation for cases where $s > 0$. For $r > 1.5$ the curves are almost independent of s and are almost linear. The interpretation is that with drag absent the slump process is restrained only by end forces and for a linear flow law the resulting flow results in a strain-rate which, for small strain, decreases linearly with increasing α . For small r drag becomes significant and the situation is more interesting. End effects, necking at the upper end and wave formation at the lower end, take place more abruptly with respect to α . (A non-linear flow law would result in even more abrupt end effects; this was observed experimentally.) For large s the curves are again almost independent of r and are almost linear for $r > 0.4$ and $s = 1$. The area under all curves is unity because of the incompressibility condition.

* Satisfactory convergence was not obtained in evaluating τ_c for the upper reservoir of Rusty Glacier, Table I.

† Pre-surge thickness magnifications of order 50 to 80% were calculated from experimental results as discussed later (see Table II). However, the calculations were based upon the assumption that the longitudinal surface strain persists at all depths. This assumption was clearly not satisfied and we estimate that the calculated values must be reduced by as much as 50%.

‡ Incompressibility implies that $\eta(\alpha, \beta, \tau) = 1/(1 + \epsilon_x(\alpha, \beta, \tau))$. The parabolic velocity profile results in

$$\epsilon_x(\alpha, \beta, \tau) = \epsilon_x(\alpha, 0, \tau)(1-\beta^2) \text{ so that } \eta(\alpha, \beta, \tau) = 1/\left[1 + \left(-1 + \frac{1}{\eta(\alpha, 0, \tau)}\right)(1-\beta^2)\right].$$

§ Those familiar with the effect of a linearized strain measure upon creep rupture-time results (Hoff, 1953; Rimrott, 1959; Shoemaker, 1965) will realize that in all these previous examples a linearized strain measure leads to a slow-down of creep (resulting in infinite creep rupture times). However, in compression, a linear strain measure leads to a speed-up in creep and in the present problem the effect of compression at the lower end dominates the effect of tension at the upper end.

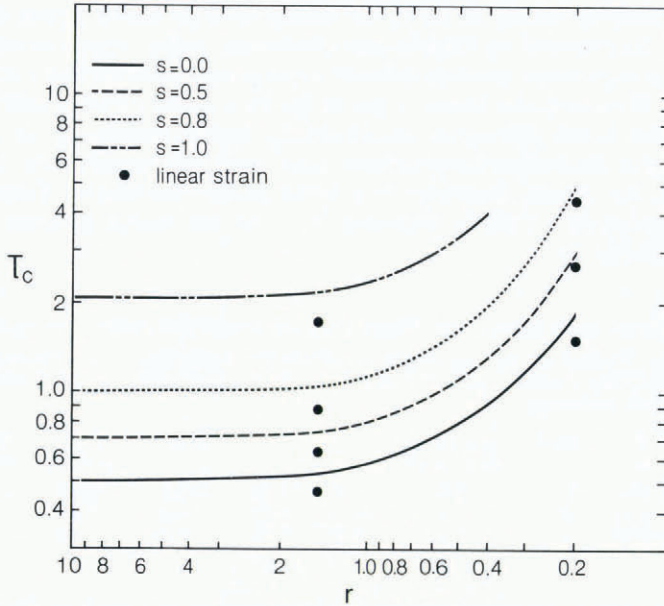


Fig. 2. Dimensionless critical time τ_c , corresponding to $\eta_0 = 1.3$, versus the drag parameter r for various values of the hydrostatic variation parameter s . The $s = 1$ curve could not be continued below $r = 0.4$ because the required small $\Delta\tau$ values resulted in excessive computation time. Seven results are plotted corresponding to a linear strain measure.

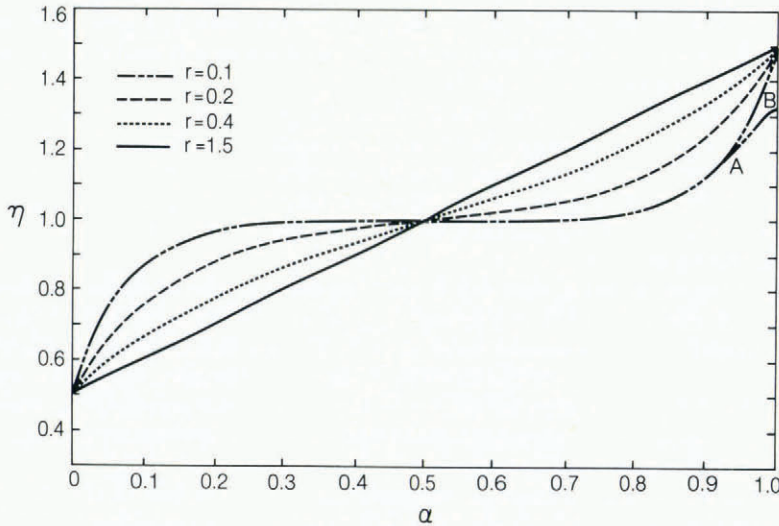


Fig. 3. Dimensionless centre-line profiles for $s = 0$ and various r values. Arc AB indicates what the profile might be in the actual situation where outflow takes place. As an indication of the effect of s , the following parameter values result in nearly identical profiles:

- (i) $s = 0.5, r = 0.2$ and $s = 0, r = 0.33$;
- (ii) $s = 0.5, r = 0.4$ and $s = 0, r = 0.6$;
- (iii) $s = 0.5, r = 0.8$ and $s = 0, r = 1.0$;
- (iv) $s = 0.8, r = 0.2$ and $s = 0, r = 0.6$;
- (v) $s = 0.8, r = 0.4$ and $s = 0, r = 0.8$.

For $s = 0.5, 0.8$, and 1.0 the curves approach a straight line for $r > 1.0, r > 0.8$, and $r > 0.4$, respectively.

Table I presents various estimates of τ_c for Rusty Glacier based upon three different reservoir possibilities. As reported by Clarke and Goodman (1975), temperature calculations based upon bore-hole temperature profiles indicate a temperate basal region 1 900 m in length (Overall in Table I). However, the lower 1 300 m lies in a narrow valley and it is not clear whether the upper and lower reservoirs would slump independently or as one reservoir. Unfortunately, as of 1970 the surface longitudinal strain field was compressive throughout the 1 900 m (Collins, 1972, fig. 4) and, therefore, in contrast to the situation on Trapridge Glacier, fails to identify the reservoir. This is probably because the slump process was not well advanced on Rusty Glacier.

TABLE I. CRITICAL SLUMP TIMES t_c FOR RUSTY GLACIER RESERVOIRS BASED UPON $\eta_c = 1.3$

Convergence was not obtained for the τ_c calculation for Upper Rusty but 3.4 is a lower bound. The μ values correspond to matching a cubic and linear flow law at a stress of 1 bar; the superscript in $t_c^{0.5}$, for example, refers to a 0.5 bar matching.

Reservoir	θ °C	l m	$\sin \delta$	$\mu \times 10^{-14}$ dyn s/cm ²	r	s	τ_c	$t_c^{0.5}$ years	$t_c^{1.0}$ years	$t_c^{1.5}$ years
Upper	-5.5	570	0.1	7.8	1.4	1.70	>3.4	>520	>130	>60
Lower	-4.5	1 370	0.1	6.3	0.23	0.47	2.4	120	31	14
Overall	-5.0	1 900	0.1	7.2	0.59	0.40	0.93	40	10	4.4

Mellor and Testa's (1969) compressive creep data at 12 bar was used to obtain μ values as follows. Coefficients k_3 in cubic creep laws $\dot{\epsilon} = k_3\sigma^3$ were determined for various temperatures from the 12 bar data. The cubic laws were assumed to apply, for example, in the range 1 bar–12 bar and linear laws $\dot{\epsilon} = k_1\sigma$ below 1 bar with k_1 values determined by equating corresponding cubic and linear laws at 1 bar. This "matching" process was performed at three stress values: 0.5, 1.0, and 1.5 bar. Shown in Table I are μ values for the 1 bar matching and critical slump times corresponding to the three matchings labelled $t_c^{0.5}$, $t_c^{1.0}$, and $t_c^{1.5}$.

Values of r , s , l , θ , and δ were estimated from the data of Goodman and others (1975) and corresponding τ_c values obtained by computer.

We feel it is unlikely that slump would take place independently in the upper and lower reservoirs because there is no constraint except for an abrupt valley narrowing. This would offer some constraint that might lead to independent slump of the upper reservoir. However, Table I indicates that the critical time of the upper reservoir is much greater than that of the lower. Hence, lower reservoir slump will dominate, with the upper reservoir, which has low drag, participating in the process.

It is thought that the surge cycle time for Rusty Glacier is about 65 years (Collins, 1972). However, for much of this interval the reservoir base would be cold and it is expected that the growth of the temperate region would occur slowly. During this growth we might assume that r remains constant; however, s would initially be large. Therefore, τ_c values also would initially be large. In addition, initial small l values would cause increased t_c values from Equation (17). It is reasonable to conclude that slump is not a significant process until the temperate base approaches a critical length.

More assistance in forming a conclusion regarding the time duration of the slump process in relation to that of the surge cycle time (sct) can be had from a consideration of Collins's evidence for Trapridge Glacier. From Collins's (1972) description of Trapridge, discussed later, it can safely be assumed that the slump process was well advanced by 1969. Let us assume that slump started in 1964. With a sct of about 40 years (Goodman and others, 1975), and assuming the next surge in 1980, the ratio of t_c to sct is about 0.4. Assuming the same ratio applies to Rusty Glacier results in a value for $t_c \approx 26$ years. The validity of the model in predicting values of t_c or sct can be partially tested by comparing "Overall" t_c values of Table I with the 26 year estimate of t_c .

FIELD OBSERVATIONS—TRAPRIDGE AND RUSTY GLACIERS

Observations by Collins (1972) on Trapridge Glacier offer remarkable qualitative agreement with Figure 3 and experimental results to be discussed later. It would be best for the reader to refer to Collins's paper but we shall quote several remarks: "Unlike Rusty Glacier, maximum flow rates are found in the middle glacier near the firn line and are considerably faster, as much as 20.5 m/year (fig. 12b). Strikingly similar to the pattern of Rusty Glacier, the lower 1.3 km is almost completely stagnant and a region of unusually strong emergence, where flow lines diverge upward from the horizontal at large angles, lies between the stagnant lower tongue and the middle zone of most rapid flow. As in Rusty Glacier, the boundary zone between the active and stagnant ice is clearly marked by a relatively narrow band of sharply increased compressive longitudinal strain-rates (fig. 12c); this corresponds to a band of sharply increased slope across the glacier, suggestive of a kinematic wave front." Collins also presents longitudinal strain data. The upper region of the reservoir is extending with the maximum strains at the upper reservoir boundary; the lower reservoir region is in compression with the maximum strains at the lower reservoir boundary.

EXPERIMENTS

Thirty-three slump experiments were run, using the apparatus shown in Figure 4, with thickened malt as the viscous substance. The reservoir region was made up of one-inch-wide (25.4 mm) aluminium channel sections (strips), one to seventeen in number, which could individually be depressed by either $\frac{1}{4}$ inch (6.35 mm) or $\frac{1}{2}$ inch (12.7 mm). (In the configuration shown all strips are depressed by $\frac{1}{2}$ inch (12.7 mm). Depression of the strips provided a means of reducing the input velocity to the reservoir as compared to the average reservoir velocity.) Various dam heights were available; however, once the experimental technique

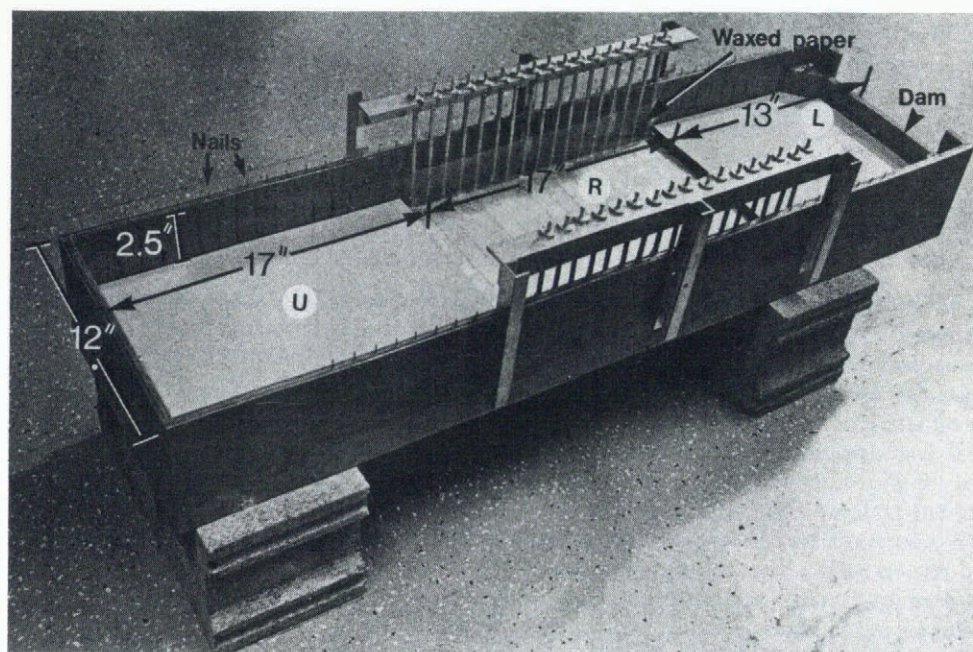


Fig. 4. Experimental trough before the addition of malt.

had been established (i.e. once we were able to produce sufficiently viscous malt) the dam never influenced the flow. Elastic bands were attached to nails and strung across the top of the trough to form a grid, as shown in Figure 5. The flow of the material with respect to this grid was measured by plastic beads floating on the malt (Fig. 5). The experiments were photographed from overhead by a 35 mm camera and the time of each photograph was recorded. Because the malt had a strong tendency to thicken with each successive test it was decided not to measure or attempt to control viscosity.

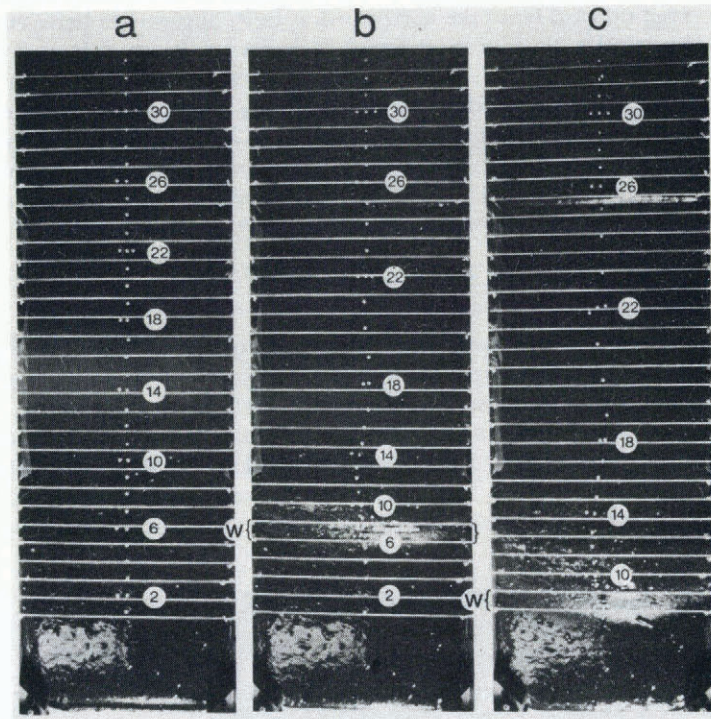


Fig. 5. Three frames from Experiment No. 8, Table II. (a) Initial configuration. (b) Just after surge initiation. Wave *W* begins to move down-stream. (c) Surge well underway with wave *W* having moved down-stream. Reflections indicate wave presence. Necked region can be seen in (c) in vicinity of bead number 25. Elapsed time between (a) and (c), 11 min.

In most experiments the aluminium strips which were to constitute the reservoir region were covered by waxed paper (Fig. 4). The waxed paper was, in turn, coated lightly with oil. (Oil was prevented from spreading outside the lubricated region by the presence of cracks between the aluminium strips. The thickness of the oil layer did not affect results. Any excess oil was pushed up the trough sides in the side-lubricated experiments. A standard light oil coat was applied in all experiments which resulted in critical slump.) Malt was then poured (or more accurately, scraped) into the trough and allowed to settle for several hours. Additional malt was added several times until a pre-determined thickness had been achieved. After equilibrium had been reached the rubber bands were attached and the plastic beads placed on top of the malt, along the centre line, at one-inch intervals. The trough was then tilted to an angle $\tan^{-1} 0.19$ and photographs taken at regular intervals. The duration of the experiments varied between one minute and twenty minutes.

With w fixed at 11 inches (279 mm), experiments were conducted with r values in the range 0.65–5.5 and s values in the range 0.03–1.9. However, the choices of r and s were found not to

be significant factors in determining whether or not slump or a surge occurred. The critical factor was found to be velocity of material entering the reservoir. Thus, if V_0 is this average velocity it was found that $V_0 t_c / l$ must be small compared to unity in order for a clearly defined slump process to occur. As $V_0 t_c / l \rightarrow 1$ the slump process became dominated by the constant-state flow through the reservoir and the only remnants of slump were a constant-state necking at the upper end of the reservoir where flow accelerates and a constant-state bulge at the lower end where flow decelerates. (Note that $V_0 t_c / l \ll 1$ for Trapridge and Rusty Glaciers.)

TABLE II. CONDITIONS FOR EXPERIMENTS WHICH RESULTED IN PRONOUNCED SLUMP (SURGE FOR THE FIRST EIGHT)

η_c values are surface centre-line values and overestimate the actual condition.

Experiment No.	Lubricated length cm	Reservoir depression mm	Height above reservoir mm	Side condition	r^\dagger	s	η_c
1	20	13	9.5	Lubricated	1.38	0.57	1.3
2	20	0	9.5	Lubricated	1.38	0.25	1.5
3	43	13	6.4	Lubricated	0.65	0.27	1.4
4	43	13	6.4	Unlubricated	0.65	0.27	1.5
5	38*	13	9.5	Unlubricated	0.73	0.39	1.7
6	43	0	9.5	Unlubricated	0.65	0.12	1.8
7	38*	13	9.5	Lubricated	0.73	0.39	1.6
8	43	0	9.5	Lubricated	0.65	0.12	1.7
9	0	13	9.5	Unlubricated	—	—	—

* One strip at each end of a 43 cm depressed region was unlubricated in order to alleviate localized end effects of the depression.

† Lubricated sides increase r values above those shown.

The remainder of our remarks will concern the nine experiments which satisfied the condition $V_0 t_c / l \ll 1$ and which did produce significant slump (Table II). The following observations and conclusions were made:

(a) All nine experiments resulted in the formation, slightly below the lower reservoir boundary, of high-amplitude waves which achieved η_c values in the range 1.5–1.8 for non-depressed reservoirs and 1.3–1.7 for depressed reservoirs (Table II). The waves were built up of small wavelets, a factor which made strain measurement extremely variable (Fig. 6). The wave profiles were much steeper than any profiles of Figure 3, probably because of the non-linear viscous behaviour of malt.

(b) Maximum pre-surge displacements of 2–4 inches (5–10 cm) were measured (Fig. 5).

(c) The first eight experiments resulted in critical conditions whereby waves abruptly detached from the reservoir and moved down-stream at a fairly constant velocity of magnitude 10–80 times that of the velocity above the reservoir. About three-quarters of the reservoir material moved down-stream in this action which we term a surge.

(d) The effect of side lubrication in experiments 1, 2, 3, 7, 8, was to produce a motion which, for fixed x , was fairly uniform except near the sides. Wave formation was fairly uniform and detachment took place uniformly and abruptly. Non-lubricated sides produced unstable flow (veering from side to side) as well as a badly skewed wave formation and non-uniform, detachment. The slump process was also significantly slower.

(e) Depressed reservoirs (experiments 1, 3, 4, 5, 7, 9) resulted in smaller η_c values (Table II) and lower velocity magnifications.

(f) Experiment 9, which can be regarded as a simulation of slump in a cold-base glacier, produced significant slump but the wave did not detach.

Figure 5 shows three frames from a typical experiment in which none of the seventeen aluminium strips were depressed (a smooth-bottomed trough) but all seventeen strips were lubricated. The initial malt thickness was $\frac{3}{8}$ in (9.5 mm). The three frames show: (i) just after tilting of the trough, (ii) just after the lower reservoir wave at W started to move down-stream, (iii) during the surge when wave W had moved down-stream.

The quantity $V_0 t_c / l$ just after the initiation of the surge, was computed from Figure 5b to be 0.016.

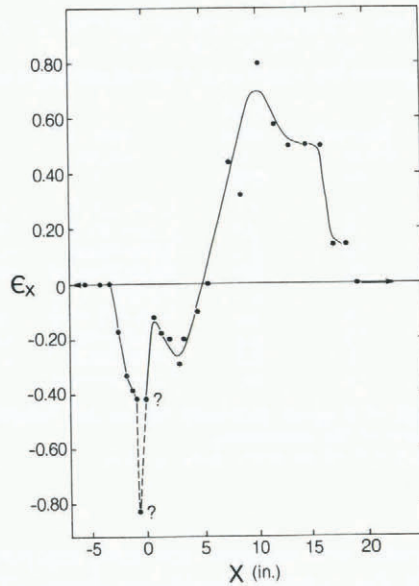


Fig. 6. Strains calculated from Figure 5b. x is the distance up-stream from lower end of reservoir.

Figure 6 shows the cumulative longitudinal strain, corresponding to critical slump, as computed from Figure 5b. Strain values tended to be erratic in the vicinity of the wave because of the folding effect mentioned earlier. (In post-surge conditions it was not uncommon for beads to become buried or for one bead to move over another. Figure 5c shows some of this confusion.)

The relation

$$\eta = 1/(1 + \epsilon_x) \quad (29)$$

can be used to relate Figures 3 and 6. These figures are not directly comparable because a strain point in Figure 6 represents cumulative strain between a bead pair which has been displaced by as much as 10 cm and therefore has moved from a tensile region toward a compressive region. This effect spreads the tensile strain region in Figure 6 to the left; Figure 6 is important mainly as an example of a rough measure of critical compressive strain.

Taking $\epsilon_x = -0.40$ from Figure 6 as a measure of maximum centre-line compressive strain, gives $\tau_c = 1.67$ from Equation (29) as compared to $\eta_c(1, 0, \tau_c) = 1.49$ of the analysis. The choice $\eta_c = 1.3$ taken from the analysis would appear to have been reasonable. Note that ϵ_x of Figure 6 is a measure of surface strain. Because the assumption of negligible longitudinal shear strain breaks down in the neighbourhood of the wave where wave spreading occurs, the large compressive strains of Figure 6 will not exist throughout the wave depth,

particularly in the case of non-depressed reservoir experiments in which longitudinal constraint to shear flow is absent at the end of the reservoir. Therefore, the η_c values of Table II are high in relation to actual average η_c values interior to the wave.

CONCLUSION

The experiments suggest that a large part of the surge-triggering mechanism in a ctc glacier is the critical wave amplitude η_c of reservoir slump. Experiments show that surges take place when $V_0 t_c / l \ll 1$. This suggests that for given V_0 slump is not of significance until the length l of the temperate reservoir grows to a critical size. In other ctc glaciers critical slump may be precluded by maximum l values which are too small.

Equation (17), used with a numerically determined value of τ_c , offers a means of predicting the critical slump time t_c of surge type ctc glaciers. In turn, t_c is a fraction of the surge cycle time and this relationship can be investigated by field studies. The quantity τ_c is only moderately dependent upon r and s in the likely range of these parameters. However, for small $r < 0.2$ and large $s > 1.0$, τ_c increases very rapidly. Therefore, combinations of small r , δ , and l and large s will tend to produce large t_c values. (Small l values would also provide small-volume surges which might not be classified as true surges.) Very large t_c values would be likely to occur in cases where the inequality $V_0 t_c / l \ll 1$ is not satisfied or otherwise might apply in situations where the evidence of past surges is blurred or non-existent. (Antarctica could be an example of the latter situation.)

Intuitively, it is easily understood that slump could be an important factor in leading to surging of temperate glaciers. All that would be required is for a broad reservoir to issue into a narrow valley. Although it represents an incomplete constraint as compared to the boundary condition of the analysis, the increased side drag of the narrow valley should favour slump. We have no data regarding the topography of any surge-type temperate glaciers which would allow us to test this conjecture. Of course, these same remarks could also apply to surging cold glaciers should any exist.

Evaluation of the model must await more field data, particularly the history of the (presumed) growth of the temperate base. It is to be hoped that some fraction of the effort currently being expended in studying surge-type temperate glaciers will in the future be directed toward ctc glaciers. In the meantime, there are additional questions which can be investigated in the laboratory: these certainly include the question of how "double reservoirs", such as exist on Rusty Glacier, interact, and might include the investigation of slump in a rapidly converging channel of a temperate glacier.

ACKNOWLEDGEMENTS

The author wishes to thank Neil Golden for assistance in running the experiments, Stan Matthews for doing the computation, and the NSERC of Canada and the Province of British Columbia for financial support.

MS. received 12 July 1978 and in revised form 20 March 1981

REFERENCES

- Clarke, G. K. C. 1976. Thermal regulation of glacier surging. *Journal of Glaciology*, Vol. 16, No. 74, p. 231-50.
 Clarke, G. K. C., and Goodman, R. H. 1975. Radio echo soundings and ice-temperature measurements in a surge-type glacier. *Journal of Glaciology*, Vol. 14, No. 70, p. 71-78.
 Collins, S. G. 1972. Survey of the Rusty Glacier area, Yukon Territory, Canada, 1967-70. *Journal of Glaciology*, Vol. 11, No. 62, p. 235-53.
 Goodman, R. H., and others. 1975. Radio soundings on Trapridge Glacier, Yukon Territory, Canada, by R. H. Goodman, G. K. C. Clarke, G. T. Jarvis, S. G. Collins, and R. Metcalfe. *Journal of Glaciology*, Vol. 14, No. 70, p. 79-84.

- Hoff, N. J. 1953. The necking and rupture of rods subjected to constant tensile loads. *Journal of Applied Mechanics*, Vol. 20, No. 1, p. 105-08.
- Isaacson, E., and Keller, H. B. 1966. *Analysis of numerical methods*. New York, John Wiley and Sons, Inc.
- Keller, H. B. 1968. *Numerical methods for two-point boundary-value problems*. Waltham, Mass., Blaisdell.
- Meier, M. F., and Post, A. S. 1969. What are glacier surges? *Canadian Journal of Earth Sciences*, Vol. 6, No. 4, Pt. 2, p. 807-17.
- Mellor, M., and Testa, R. 1969. Creep of ice under low stress. *Journal of Glaciology*, Vol. 8, No. 52, p. 147-52.
- Morland, L. W., and Johnson, I. R. 1980. Steady motion of ice sheets. *Journal of Glaciology*, Vol. 25, No. 92, p. 229-46.
- Nye, J. F. 1959. The motion of ice sheets and glaciers. *Journal of Glaciology*, Vol. 3, No. 26, p. 493-507.
- Rimrott, F. P. J. 1959. Creep of thick-walled tubes under internal pressure considering large strains. *Journal of Applied Mechanics*, Vol. 26, No. 2, p. 271-75.
- Robin, G. de Q. 1955. Ice movement and temperature distribution in glaciers and ice sheets. *Journal of Glaciology*, Vol. 2, No. 18, p. 523-32.
- Scheidegger, A. E. 1975. *Physical aspects of natural catastrophes*. Amsterdam, Elsevier Scientific Publishing Co.
- Shoemaker, E. M. 1965. Creep rupture of rotating disks and thin shells of revolution. *Transactions of the American Society of Mechanical Engineers. Ser. E. Journal of Applied Mechanics*, Vol. 32, No. 3, p. 607-10.